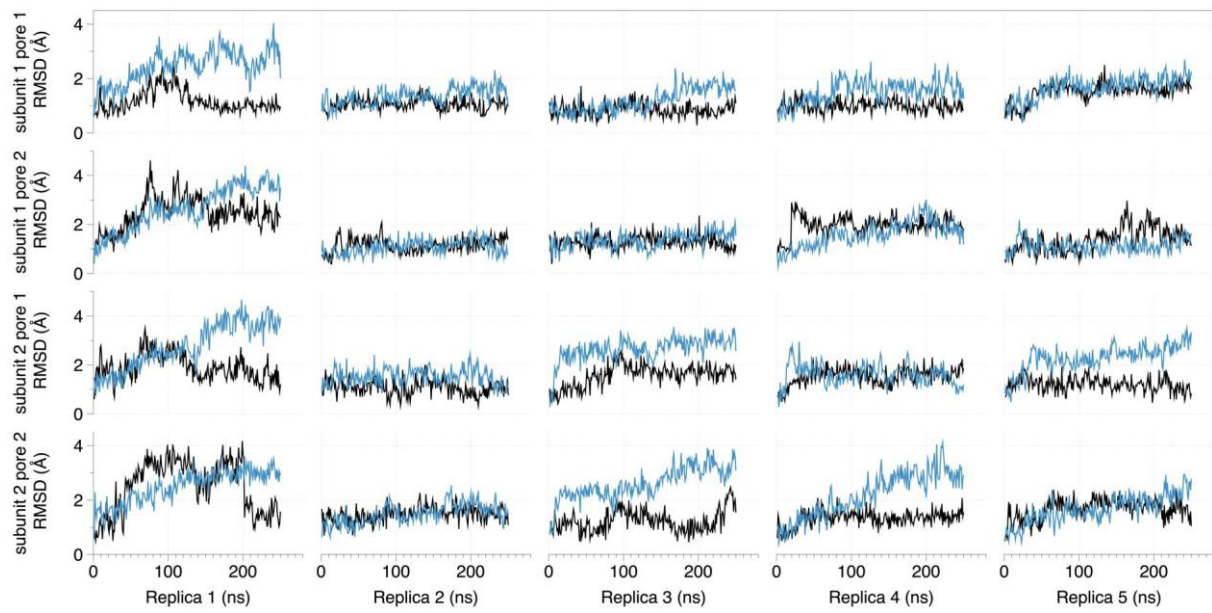


## Supplementary Figure S1



**Figure S1.** Structural stability of the selectivity filter. Analysis of root-mean-square deviation (RMSD) of the backbone of residues forming the selectivity filter of AtTPC1 in the presence of 0.15 M KCl (black) and 0.15 M NaCl (blue).

## Supplementary Figure S2

	AtTPC1-D269	AtTPC1-E637	
Medicago_truncatula_Medtr2g090380.1	NLILAVVYDSFKSELV	[...]	
Arabidopsis_thaliana_AT4G03560.1	NLILAVVYDSFKEQLA	[...]	
Vitis_vinifera_GSVIVT01020549001	NLILAVIYDSFKNQLA	[...]	NNWQVWMQSYYKDLT
Chenopodium_quinoa_LOC110703516	NLILAVVYDSFKSELA	[...]	GNWQAWMOTYWDLT
Chenopodium_quinoa_LOC11068197	NLILAVVYDSFKSELA	[...]	GNWQAWMOTYWDLT
Populus_trichocarpa_Potri.013G131100.2	NLILAVVYDSFKDQIV	[...]	GNWHEWMQSYYKDLT
Nicotiana_tabacum_Nitab4.5-0000512g0020.1	NLILAVVYDSFKSELV	[...]	GNWQVWMQSYYKELT
Aquilegia_cerulea_Aqcoe4G103300.1	NLILAVVYDSFKEQLV	[...]	GNWQVWMEGYKELT
Spirodela_polyrhiza_Spipl04G0028300	NLILAVVYDSFKAQLA	[...]	GNWQVWMESYRDLT
Oryza_sativa_LOC_Os01g48680.1	NLILAVIYDSFKEQLA	[...]	GNWQAWMESYRQLT
Salvinia_cucullata_Sacu-v1.1-s0093.g019069	NLILAVVYDSFKDQLA	[...]	GNWQVWLIESFVILT
Blechnum_spicant_scaffold-VITX-2006239	NLILAVVYDSFKEQLA	[...]	GNWQVWLIESYVLT
Thuidium_delicatulum_scaffold-EEMJ-2039009	NLILAVVYDSFKGQLA	[...]	GNWEVWMDFGFLEVT
Physcomitrella_patens_Pp3c15-12230V3.1	NLVLAVVYDSFKGQLA	[...]	GNWHIWMDFGQEVT
Sphagnum_fallax_Sphfalx04G006400.1	NLILAVVYDSFKGQLA	[...]	GNWQVWMGGYAQLT
Takakia_lepidoziooides_scaffold-SKQD-2009335	NLILAVVYDSFKGQLA	[...]	SNWEVEMDGYAELT
Physcomitrella_patens_Pp3c1-6272V3.1	NLILAVVYDSFKGQLA	[...]	GSWQTWMDSYVVLT
Physcomitrella_patens_Pp3c1-6270V3.1	NLILAVVYDSFKGQLA	[...]	GSWQTWMDSYVVLT
Thuidium_delicatulum_scaffold-EEMJ-2007306	NLILAVVYDSFKGQLA	[...]	GNWQSWMDSFVILT
Marchantia_polymorpha_Mapoly0002s0274.1	NLILAVVYDSFKGQLA	[...]	GNWQVWMETYGILS
Nothoceros_vincentianus_scaffold-TCBC-2005470	NLILAVVYNDFKEQFA	[...]	GNWQIWMESYAHLT
Klebsormidium_nitens_kf100312-0080-v1.1	NLILAVIYDSFQKQLG	[...]	ADWQDWMEGYAILG
Klebsormidium_nitens_kf100110-0290-v1.1	NLILAVIYDSFKNQLG	[...]	ASWQDWMEGYAVLS
Klebsormidium_nitens_kf100097-0180-v1.1	SLILAVVYNGYKDQIT	[...]	TLYSDWQSIASNIY
Klebsormidium_nitens_kf100001-0210-v1.1	SLILAVVYDGYKNSLA	[...]	SLFSVWLTIAGRIY
Klebsormidium_nitens_kf100012-0290-v1.1	NLILAVIYDAFKEQVV	[...]	SSWILTYQDAFVRAT
Chara_australis_CL6562.Contig1-All.p1	SLLFSVVERGYQRQLA	[...]	RDWIVFAKGYVAAT
Marchantia_polymorpha_Mapoly0050s0061.1	HLLFALIYNNYKVQLA	[...]	NNWYVIMDGIVAAS
Marchantia_polymorpha_Mapoly0062s0036.1	NVAFAVIYTTFKRMQA	[...]	GNWYIIMEGYSAAT
Physcomitrella_patens_Pp3c3-16950V3.1	NLVEFTVIYSNYKAQMV	[...]	NNWVYEMDAYAVAT
Takakia_lepidoziooides_scaffold-SKQD-2009261	NLVFSVIYSNYKAQIA	[...]	NNWYVEMDAYAAAT
Sphagnum_fallax_Sphfalx16G086000.1	NLAFMVIIYSNYKVEIA	[...]	NNWYVIMDAYAFVT
Sphagnum_fallax_Sphfalx19G080400.1	NFAFTVIYSSYKAQIA	[...]	NNWVYIMDAYAIVT
Sphagnum_fallax_Sphfalx03G070700.1	NLAFSVIYSNYKAQMA	[...]	NKWWVYEMDAYAAVT
Buxbaumia_aphylla_scaffold-HRWG-2017281	NLAFSVIYSSYKAQMA	[...]	NKWWYVFMDAYAAVT
Physcomitrella_patens_Pp3c19-18680V3.1	NLAFSLIYSNYKAQMA	[...]	NKWWVYFMDAYAAVT
Thuidium_delicatulum_scaffold-EEMJ-2039845	NLAFSVIYSSYKQOMA	[...]	NKWWVYEMDAYAAVT
Physcomitrella_patens_Pp3c18-10190V3.1	NLAFSVIYSSYKAQMA	[...]	NKWWVYEMDAYAAVT
Physcomitrella_patens_Pp3c21-11410V3.1	NLAFSVIYSSYKAQMA	[...]	NKWWVYIMDAYAAVT
Takakia_lepidoziooides_scaffold-SKQD-2080274	NLVFSVIYSNYKAQMA	[...]	NKWWVIMDAYAVAT
Sphagnum_fallax_Sphfalx16G017900.1	SLAFSVVYNSYKSQMV	[...]	NKWWVIMDAYAAAT
Buxbaumia_aphylla_scaffold-HRWG-2013254	NLAFSVIYSNYKAQMA	[...]	NKWWVIMDGFAAAA
Physcomitrella_patens_Pp3c14-20770V3.1	NLAFSVVYNSYKTQMA	[...]	NKWWVIMDGYAAAT
Physcomitrella_patens_Pp3c1-28370V3.1	NLAFSVVYNSYKAQMA	[...]	NKWWVIMDGYAAAT
Physcomitrella_patens_Pp3c2-10230V3.1	NLAFSVIYSNYKAQMA	[...]	NKWWVIMDGYAAAT

**Figure S2.** Sequence comparison of TPC1s from different species. Shown are the regions around AtTPC1-D269 and AtTPC1-E637. Sequence data are from [9].

### **Supplementary Figure S3**

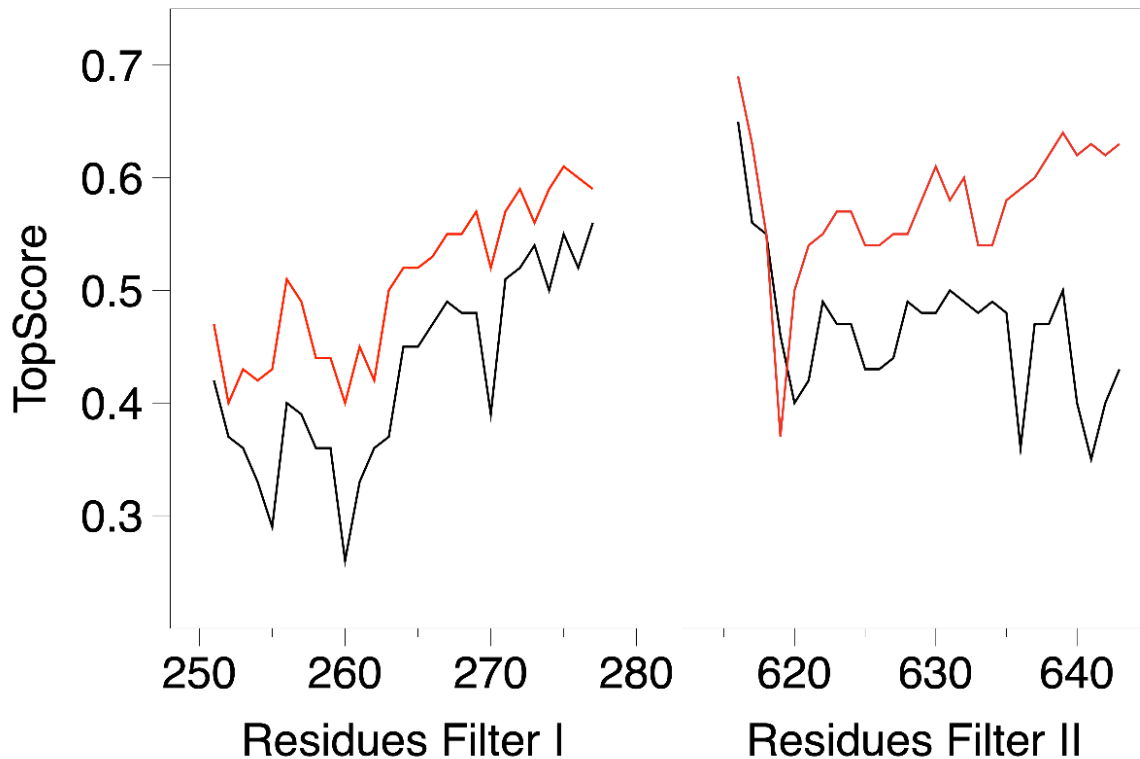


**Figure S3.** Per-residue TopScore of the filter regions in the AtTPC1 crystal structure of the closed configuration (black) and in the model of the open configuration (red). TopScore [55] provides a meta quality assessment of the protein structure at the global and per-residue level by estimating the error in a scale from 0 to 1. There is only a moderate increase in the estimated error between the crystal closed configuration and the modelled open configuration. The largest differences are observed for the selectivity filter residues in the second domain of AtTPC1. These residues are located in the vicinity of the IIS6 helix, which is the helix responsible for channel opening.